Article:
Fagernäs, Zandra, García-Collado, Maite I., Hendy, Jessica orcid.org/0000-0002-3718-1058 et al. (4 more authors) (2020) A unified protocol for simultaneous extraction of DNA and proteins from archaeological dental calculus. Journal of archaeological science. 105135. ISSN 0305-4403

https://doi.org/10.1016/j.jas.2020.105135

Journal of Archaeological Science 118 (2020) 105135

Contents lists available at ScienceDirect

Journal of Archaeological Science

journal homepage: http://www.elsevier.com/locate/jas

A unified protocol for simultaneous extraction of DNA and proteins from archaeological dental calculus

Zandra Fagernäs [a], Maite I. García-Collado [b], Jessica Hendy [a,c], Courtney A. Hofman [d,e], Camilla Speller [c,f], Irina Velsko [a], Christina Warinner [a,g,h,*]

[a] Department of Archaeogenetics, Max Planck Institute for the Science of Human History, Jena, 07745, Germany
[b] Department of Geography, Prehistory and Archaeology, University of the Basque Country, Leioa, 48940, Spain
[c] Department of Archaeology, University of York, York, YO10 5NG, United Kingdom
[d] Department of Anthropology, University of Oklahoma, Norman, 73019, United States
[e] Laboratories of Molecular Anthropology and Microbiome Research, University of Oklahoma, Norman, 73019, United States
[f] Department of Anthropology, University of British Columbia, Vancouver, V6T 1Z4, Canada
[g] Department of Anthropology, Harvard University, Cambridge, 02138, United States
[h] Faculty of Biological Sciences, Friedrich Schiller University, Jena, 07743, Germany

ARTICLE INFO

Keywords:
Ancient DNA
Palaeoproteomics
Oral microbiome
Dental plaque
Metagenomics

ABSTRACT

Archaeological materials are a finite resource, and efforts should be made to minimize destructive analyses. This can be achieved by using protocols combining extraction of several types of biomolecules or microparticles, which decreases the material needed for analyses while maximizing the information yield. Archaeological dental calculus is a source of several different types of biomolecules, as well as microfossils, and can tell us about the human host, microbiome, diet, and even occupational activities. Here, we present a unified protocol allowing for simultaneous extraction of DNA and proteins from a single sample of archaeological dental calculus. We evaluate the protocol on dental calculus from six individuals from a range of time periods and estimated preservation states, and compare it against previously published DNA-only and protein-only protocols. We find that most aspects of downstream analyses are unaltered by the unified protocol, although minor shifts in the recovered proteome can be detected, such as a slight loss of hydrophilic proteins. Total protein recovery depends on both the amount of starting material and choice of extraction protocol, whereas total DNA recovery is significantly reduced using the unified protocol (mean 43%). Nevertheless, total DNA recovery from dental calculus is generally very high, and we found no differences in DNA fragment characteristics or taxonomic profile between the protocols. In conclusion, the unified protocol allows for simultaneous extraction of two complementary lines of biomolecular evidence from archaeological dental calculus without compromising downstream results, thereby minimizing the need for destructive analysis of this finite resource.

1. Introduction

Biomolecular analysis is becoming increasingly feasible in archaeology as methods improve and costs decrease. However, archaeological materials are a finite resource, and there is a need to develop techniques that reduce the extent of destructive sampling, while concurrently maximizing the amount of information that can be obtained (Green and Speller, 2017). So-called non-destructive methods for extracting DNA (Bolnick et al., 2012; Rohland et al., 2004) and proteins (Fiddyment et al., 2015; Manfredi et al., 2017; van Doorn et al., 2011) from ancient materials have been developed, but many of these techniques are limited by downstream challenges, including lower or biased biomolecule recovery, higher rates of contamination, and a higher burden of sample degradation. Depending on the research question and the sample type, such techniques may not be suitable. Alternatively, it is possible to modify existing destructive methods to either simultaneously or sequentially extract multiple classes of biomolecules (e.g., DNA, proteins, lipids, metabolites) from the same specimen, thereby taking advantage of the effectiveness of destructive methods while improving efficiency and minimizing waste. Such an approach has previously been applied with success to combining methods for genetic analysis and radiocarbon dating of skeletal remains (Korlević et al., 2018) and to

* Corresponding author. Department of Archaeogenetics, Max Planck Institute for the Science of Human History, Jena, 07745, Germany.
E-mail address: warinner@shh.mpg.de (C. Warinner).

https://doi.org/10.1016/j.jas.2020.105135
Received 8 January 2020; Received in revised form 25 March 2020; Accepted 25 March 2020
Available online 24 April 2020

combining lipid analysis and radiocarbon dating (Berstan et al., 2008; Casanova et al., 2018).

Developing a unified protocol to recover multiple classes of biomolecules also presents several research advantages. Less material is required for analysis, which reduces sampling demands and mitigates variability that can arise from heterogeneous substrates. In addition, different classes of biomolecules can provide distinct but complementary lines of analysis, thereby strengthening the results of a study. For example, two studies of ancient dental calculus (Velsko et al., 2019; Warinner et al., 2014b) identified both DNA and proteins from the periodontal pathogen *Porphyromonas gingivalis*, thereby providing strong evidence of both its presence and activity. For highly degraded samples, targeting multiple classes of biomolecules also improves the chances of retrieving at least one successfully (Chen et al., 2019). DNA and proteins are known to have considerably differing maximum ages of survival, with proteins surviving for millions of years (Demarchi et al., 2016), whereas the oldest successfully recovered DNA, even from permafrost, is less than a million years old (Orlando et al., 2013). However, regardless of age, it can be difficult to accurately predict the analytical success of a given sample in advance, as the preservation of individual specimens can be highly dependent on local environmental factors.

One archaeological substrate for which a unified extraction protocol would be particularly useful is dental calculus. Archaeological dental calculus is a rich source of ancient biomolecules (e.g., DNA, proteins, metabolites) and microremains (e.g., plant microfossils, environmental debris) that originate from the host, microbes, food, and the environment (Radini et al., 2017; Velsko and Warinner, 2017). Forming through periodic calcification of dental plaque, dental calculus entraps and preserves such debris throughout an individual's lifetime, and it can persist over very long periods of time due to its densely mineralized nature. From a single sample of calculus, it is possible to gain information about the individual's genome (Ozga et al., 2016; Ziesemer et al., 2019), oral microbiome and health (Velsko et al., 2019, 2017; Warinner, 2016; Warinner et al., 2014b), diet (Hendy et al., 2018; Jeong et al., 2018; Warinner et al., 2014a), and even occupational activities (Radini et al., 2019). Nevertheless, the amount of dental calculus available per individual is typically low (on the order of tens of milligrams), which limits the number of biomolecule extractions, and therefore analyses, that can be performed.

Efficient protocols have been developed to isolate different types of biomolecules and microremains from ancient dental calculus, including DNA and proteins (Jeong et al., 2018; Mann et al., 2018), as well as phytoliths and starch granules (Henry and Piperno, 2008; Tromp et al., 2017). Currently, however, many of these protocols are incompatible. For example, calculus decalcification using HCl (for microfossil extraction) is incompatible with DNA analysis; strong heat denaturation (for protein extraction) is incompatible with DNA and starch granule analysis; use of proteinase K (for DNA extraction) is incompatible with protein analysis. DNA and protein extraction protocols are the most difficult to combine, as they typically involve multiple incompatible steps. Previous attempts have been made to modify and combine DNA and protein extraction protocols for archaeological teeth (Rusu et al., 2019) and dental calculus (Mackie et al., 2017); however, in each case the performance and efficiency of the combined protocol was not compared to similar, non-combined protocols. As such, the efficiency and potential biases of the combined protocols could not be systematically evaluated.

Here we present a unified protocol (UP) for the simultaneous extraction of DNA and proteins from archaeological dental calculus. This protocol is based on prior observations from genomic and proteomic experiments that, following decalcification, most DNA is recovered from the supernatant rather than the cell pellet, while most protein is recovered from the cell pellet rather than the supernatant. We evaluate the performance of the UP on a panel of dental calculus specimens originating from archaeological sites of different antiquities and estimated preservation states, and we apply the protocol to both high (10 mg) and low (2 mg) starting amounts of dental calculus. We then compare these results to those obtained using DNA-only (DO) and protein-only (PO) protocols in order to assess the efficiency of the UP and identify potential biases. We evaluate the UP on the basis of total DNA and protein recovery, DNA fragment length, DNA GC-content, amino acid properties, protein hydropathy and molecular weight, reconstructed microbiome, proteome composition, and contamination burden. Overall, we find that the UP introduces relatively few biases and is a more efficient use of starting material than performing separate DO and PO extractions. Only DNA recovery is strongly impacted, with the UP resulting in a 43% lower DNA yield on average compared to the DO protocol, which we propose is due to the absence of proteinase K during the initial separation of DNA following decalcification. Nevertheless, given that ancient dental calculus typically contains high amounts of DNA in excess of metagenomic sequencing requirements (Mann et al., 2018), this reduction in DNA recovery is unlikely to limit downstream investigations in most cases.

2. Methods

2.1. Sample material

Dental calculus samples were obtained from four archaeological sites representing different time periods and estimated preservation states (Table 1). Calculus samples from Driffield Terrace and Wighill had been previously analyzed and shown to have good protein preservation (Hendy et al., 2018; Mackie et al., 2017; Warinner et al., 2014a), while calculus samples from Rupert's Valley had been previously shown to have poor DNA preservation and a high contamination burden from environmental bacteria (Ziesemer et al., 2015). Calculus from San Martín de Dulantzi had not been previously analyzed using molecular techniques. In total, dental calculus from six individuals was analyzed in this study: one individual each from Driffield Terrace, Wighill and Rupert's Valley, and three individuals from San Martín de Dulantzi.

2.2. Laboratory procedures

All DNA and protein extractions were performed in dedicated

Table 1
Dental calculus samples analyzed in this study.

Sample ID	Archaeological ID	Site	Age	Preservation
Yorkshire, England				
DRT001	3DT21	Driffield Terrace	44-410 CE	Good
WIG001	WG1561	Wighill	1000–1550 CE	Good
Basque Country, Spain				
SMD017	SMD 1441-1-1440(044)	San Martín de Dulantzi	700–950 CE	Unknown
SMD046	SMD 2591-1-2590(159)	San Martín de Dulantzi	700–950 CE	Unknown
SMD051	SMD 2711-1-2710(171)	San Martín de Dulantzi	700–1150 CE	Unknown
St. Helena, South Atlantic Ocean				
RUV001	SK203	Rupert's Valley	1840–1872 CE	Poor

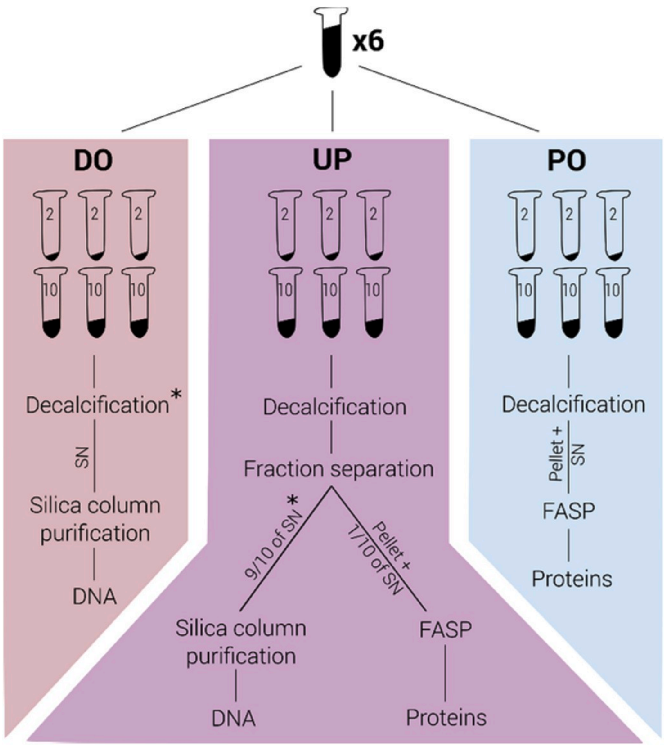

Fig. 1. Flowchart of extraction protocols and experiments. Amount of starting material is in milligrams. The asterisk denotes addition of proteinase K and 'SN' indicates supernatant.

archaeogenetic and palaeoproteomic facilities at the Max Planck Institute for the Science of Human History (Jena, Germany). DNA-only (DO) and protein-only (PO) extractions were performed alongside the unified (UP) extractions, and sample batches were randomized to avoid batch effects. For all extractions, two sample starting weights were used, 2 mg and 10 mg, in order to investigate the efficiency of the protocols on different amounts of starting material. Extractions for each sample, protocol, and starting weight were performed in triplicate (Fig. 1), resulting in a total of 72 DNA extracts and 72 protein extracts.

2.2.1. Sample collection and preparation

Dental calculus was collected from archaeological teeth using a sterile dental scaler and UV irradiated for 2 min to reduce potential surface contamination. Calculus from each individual was homogenized for 5 s at 20 Hz in an oscillating mill (MM200, Retsch) using 15 mm zirconium oxide beads. The resulting powder was subsampled for use in all subsequent extractions. Only nitrile gloves were used during sample processing, as latex gloves may introduce latex proteins into the samples.

2.2.2. DNA-only (DO) protocol

DNA extraction was performed following Dabney et al. (2013), with modifications adapted for dental calculus (Mann et al., 2018). Briefly, the powdered dental calculus was washed with 1 ml of 0.5 M EDTA to remove surface contaminants, and the supernatant was removed without incubation. The remaining dental calculus was decalcified in 1 ml of 0.5 M EDTA on a rotator at room temperature for 24 h, after which 50 μl of 10 mg/ml proteinase K (Sigma-Aldrich) was added. The samples were further decalcified for 48 h by rotation at room temperature (total decalcification time 72 h), followed by centrifugation at 18400 rcf for 1 min to pellet cell debris. The complete supernatant was then removed and mixed with 10 ml binding buffer (5 M guanidine hydrochloride, 0.12 M sodium acetate and 40% isopropanol). DNA purification was performed using the High Pure Viral Nucleic Acid kit (Roche Life Science) following the manufacturer's instructions. DNA was eluted from the column in two rounds of 50 μl of Qiagen EB buffer, to which Tween 20 had been added to a final concentration of 0.05%. DNA quantification was performed on 1 μl of the eluate with a Qubit HS assay (Thermo Fisher Scientific). DNA extractions were performed in batches of 3–12 samples, and one extraction blank was included per batch.

2.2.3. Protein-only (PO) protocol

Protein extraction and digestion was performed using a filter-aided sample preparation (FASP) protocol (Wiśniewski et al., 2009) modified for ancient dental calculus (Jeong et al., 2018). Briefly, the powdered dental calculus was decontaminated as described in section 2.2.2., and then decalcified in 1 ml of 0.5 M EDTA on a rotator at room temperature for 72 h. After decalcification, the samples were centrifuged at 18400 rcf for 1 min to pellet cellular material, and 200 μl of supernatant was transferred to a 30 kDa Microcon filter unit (Merck) containing 50 μl of 8 M urea. The mixture was centrifuged through the filter at 14000 rcf for 10 min. This procedure was repeated until all supernatant had been passed through the filter. The pellet was resuspended in 30 μl of lysis buffer (containing 4% w/v sodium dodecyl sulfate, 100 mM Tris hydrochloride and 0.1 M dithiothreitol) and incubated at 95 °C for 5 min, followed by centrifugation at 14000 rcf for 1 min to pellet cell debris. The supernatant was then mixed with 200 μl of 8 M urea, transferred to the corresponding Microcon filter unit used in the previous step, and centrifuged at 14000 rcf for 20 min. The filter was washed with 200 μl of 8 M urea in an additional centrifugation step. On the filter, proteins were alkylated by adding 100 μl of 0.5 M iodoacetamide solution and incubating for 5 min at room temperature in the dark. The filter units were then centrifuged at 14000 rcf for 12 min, and washed twice with 100 μl of 8 M urea and twice with 100 μl of 0.5 M NaCl. The proteins were digested overnight at 37 °C on the filter in a digestion buffer consisting of 117 μl of 0.05 M triethylammoniumbicarbonate and 3 μl of 0.4 μg/μl porcine trypsin (Pierce Trypsin Protease MS Grade, Thermo Fisher Scientific). Digested peptides were recovered from the filter by centrifugation at 14000 rcf, and acidified by adding 5% trifluoroacetic acid (TFA) to get a final concentration of 0.5% TFA. The acidified peptides were desalted using StageTips (C18 tips, Thermo Fisher Scientific) following the manufacturer's instructions, and dried to completion in a vacuum centrifuge (Martin Christ RVC 2-18). Protein quantification was performed by rehydrating the peptides in 20 μl of 3% acetonitrile/0.1% TFA and measuring the absorbance at 215 nm with a spectrophotometer (DeNovix DS-11 FX+). Afterwards, the samples were dried to completion in a vacuum centrifuge and stored at −80 °C until further analysis. Protein extraction and digestion was performed in batches of 12–24 samples, and one extraction blank was included per batch.

2.2.4. Unified protocol (UP)

Powdered dental calculus samples were decontaminated as described in section 2.2.2., and then decalcified in 1 ml of 0.5 M EDTA on a rotator at room temperature for 72 h. After decalcification, the samples were centrifuged at 18400 rcf for 1 min to pellet cellular material, and 900 μl of supernatant was transferred into a new tube containing 50 μl of 10 mg/ml proteinase K (Sigma-Aldrich) and incubated overnight at room temperature. To this, 10 ml binding buffer (5 M guanidine hydrochloride, 0.12 M sodium acetate and 40% isopropanol) was added, and DNA was purified and quantified using the method described in section 2.2.2. Proteins were extracted, digested and quantified from the remaining 100 μl supernatant and cell debris pellet using the modified FASP protocol as described in section 2.2.3. Unified extractions were performed in batches of 11–13 samples, and one extraction blank was included per batch.

2.2.5. DNA sequencing

One randomly selected DNA extract per individual per protocol (DO2, DO10, UP2 and UP10; 24 in total), as well as blanks from

extractions and library preparations (9 in total), were treated with partial uracil-DNA glycosylase treatment (Rohland et al., 2015) and prepared into double-stranded DNA libraries with dual indexing following published protocols (Kircher et al., 2012; Meyer and Kircher, 2010) using 20–25 μl extract each. The libraries were normalized and pooled in equimolar amounts and sequenced on an Illumina NextSeq with 75-bp paired-end chemistry to a depth of approximately 10 million reads for calculus samples and 2 million reads for blanks.

2.2.6. LC-MS/MS

Liquid chromatography tandem mass spectrometry (LC-MS/MS) was performed on one randomly selected protein digest per individual per protocol (PO2, PO10, UP2 and UP10; 24 in total), as well as extraction blanks (3 in total), at the Functional Genomics Centre Zürich (University of Zürich, Switzerland). The samples were analyzed on a Q-Exactive HF mass spectrometer (Thermo Fisher Scientific) coupled to an ACQUITY UPLC M-Class system (Waters AG), following the procedures and parameters described in Jeong et al. (2018).

2.3. Analysis workflow

Statistical analysis was performed in R v. 3.6.1 (R Core Team, 2018). Differences between protocols were tested with pairwise Wilcoxon tests and corrected for multiple testing using the Benjamini-Hochberg method (hereafter called pW-BH), unless otherwise noted. General R-packages used for data manipulation and creating graphical figures were tidyverse v. 1.2.1 (Wickham, 2017), janitor v. 1.2.0 (Firke, 2018), ggpubr v. 0.2.3 (Kassambara, 2018), gtools v. 3.8.1 (Warnes et al., 2018), ggsignif v. 0.6.0 (Ahlmann-Eltze, 2019), cowplot v. 1.1.0 (Wilke, 2017), rcartocolor v. 2.0.0 (Nowosad, 2018) and fuzzyjoin v. 0.1.4 (Robinson, 2018). Individual RUV001 was excluded from all statistical tests after it was found to exhibit a non-typical DNA and protein composition for calculus (indicating very poor preservation), however, results for this individual are shown in figures. R Markdown files for all analyses are available on GitHub (https://github.com/ZandraFagernas/unified_protocol).

2.3.1. Genetic analysis

2.3.1.1. DNA recovery. DNA yield was normalized by starting weight of dental calculus. The values were log-transformed, and linear mixed-effect models with the individual as the random effect were fitted to find the model that best predicts DNA recovery. All mixed effects models were fit using the R-package lme4 v. 1.1.21 (Bates et al., 2015), model selection tests via ANOVA were performed using the R-package lmerTest v. 3.1.0 (Kuznetsova et al., 2017) and Box-Cox transformations were identified using the R-package MASS (Venables and Ripley, 2002).

2.3.1.2. Data preprocessing. EAGER v.1.92.55 (Peltzer et al., 2016) was used to process the raw DNA reads and align sequences to the human reference genome (HG19). In this pipeline, adapter removal and read merging were performed by AdapterRemoval v. 2.2.0 (Schubert et al., 2016). On average, 87.3 ± 7.8% (mean ± standard deviation) of calculus reads and 36.8 ± 23.6% of blank reads merged. BWA v. 0.7.12 (Li and Durbin, 2009) was used for human genome alignment with default settings (-l 32, -n 0.01) without quality filtering. Unmapped reads were extracted with SAMtools v. 1.3 (Li et al., 2009) for downstream processing, and duplicates removed using DeDup v. 0.12.2 (Peltzer et al., 2016). Non-human reads were aligned to the NCBI nucleotide database (as of April 2016) using MALT v. 0.3.8 (Herbig et al., 2016) to assign taxonomy (settings –minPercentIdentity 85.0, –topPercent 1.0, –minSupportPercent 0.01). MEGAN v. 6.11.1 (Huson et al., 2016) was used to export genus- and species-level OTU-tables with summarized read counts from the MALT results.

2.3.1.3. Fragment characteristics. For calculations of GC-content and fragment length, adapter-trimmed, merged reads were aligned to *Actinomyces oris* strain T14V (NCBI assembly accession ASM155393v1) and *Leptotrichia buccalis* strain DSM 1135 (NCBI assembly accession ASM2390v1) using the EAGER pipeline described above, with the exception of mapping quality being set to 37. These oral bacterial species were chosen due to their high abundance in the samples, as well as their differential median GC-content (*A. oris* 68.3%, *L. buccalis* 29.6%).

2.3.1.4. Microbiome reconstruction. The R-package decontam v. 1.1.2 (Davis et al., 2018) was used to identify putative contaminants from genus- and species-level OTU tables. The prevalence method was used (with default threshold = 0.1) to identify OTUs with a higher prevalence in blanks than in samples, thereby likely being contaminants. A species-level OTU-table, with putative contaminants removed, was used to investigate the taxonomic profiles of the samples. The 20 most abundant species across all samples were calculated excluding individual RUV001, and the abundance of these species was compared across extraction protocols. The body site these species are associated with was extracted from the expanded Human Oral Microbiome Database (eHOMD; Escapa et al., 2018). A principal component analysis was conducted on a genus-level OTU-table, after multiplicative zero replacement using the R-package zCompositions v. 1.3.2.1 (Palarea-Albaladejo and Martín-Fernández, 2015) and CLR-transformation (Gloor et al., 2017). The two loadings with highest contribution to the separation along each PC in both the negative and positive directions were extracted and added to the PCA plots. A PERMANOVA (Anderson, 2001) was performed on the dataset without RUV001 using the 'adonis' function (on Euclidean distances with 999 permutations) from the R-package vegan v. 2.5–6 (Oksanen et al., 2019), in order to assess drivers of variation in microbiome composition.

2.3.1.5. Contamination. The species that were identified as putative contaminants (described in section 2.3.1.4) were further analyzed to evaluate if the proportion and composition of contaminants differed between extraction protocols.

2.3.2. Proteomic analysis

2.3.2.1. Protein recovery. Protein yield was normalized by starting weight of dental calculus. The values were log-transformed, and linear mixed-effect models were fitted in order to find the model that best predicts protein recovery, as described in section 2.3.1.1 .

2.3.2.2. Data preprocessing. MSConvert v. 3.0.11781 (ProteoWizard) was used to transform raw data files (.raw) to Mascot generic files (.mgf), using the 100 most intense peaks. The resulting files were searched using Mascot v. 2.6.0 (Matrix Science) against the Swiss-Prot database (as of January 2018) plus reversed decoys (in total 1.1 million entries). Fragment ion mass tolerance was set to 0.01 Da and parent ion tolerance to 10.0 ppm. Carbamidomethylation C was set as a fixed modification, and deamidation (N and Q) and oxidation (M and P) as variable modifications (Hendy et al., 2018; Jeong et al., 2018). Using Scaffold v. 4.8.9 (Proteome Software Inc.), the results were filtered to a 1% peptide false discovery rate (FDR), a 5% protein FDR, and a minimum support of two peptides. Decoy hits and common laboratory contaminants (collagen, keratin and serum albumin) were removed before subsequent analyses. The resulting dataset was exported from Scaffold at the levels of peptides, proteins, and protein clusters, to be used in downstream analyses.

2.3.2.3. Protein characteristics. Hydropathy values (a measure of hydrophobicity) were calculated for recovered proteins using the web application GRAVY Calculator (www.gravy-calculator.de/). Molecular weights of all identified proteins were obtained from the protein report file exported from Scaffold. Physicochemical properties of amino acids

were calculated using the R-package Peptides v. 2.4 (Osorio, 2015) from all unique identified peptides.

2.3.2.4. Proteome reconstruction. Scaffold was used to annotate protein clusters with gene ontology (GO) terms from NCBI (as of May 2019). Protein clusters were selected because this groups proteins by homology and functional similarity, thereby mitigating some of the uncertainty introduced by assigning proteins to species. The GO terms for cellular location were classified into three groups: 1) intracellular and organelle, 2) membranes, and 3) extracellular. Protein clusters with GO terms for more than one of these groups were classified as: 4) Various; clusters without GO terms for cellular location available were classified as: 5) Unknown. The top 20 most abundant protein clusters were calculated excluding RUV001. A table of the percentage of total spectra belonging to each protein cluster per individual was used as input for a PCA. Only protein clusters present in at least two of the samples were included, and the data was log2-transformed after pseudocount zero replacement (+1). The two loadings with highest contribution to separation along each PC in positive and negative directions were added to the PCA plots. Drivers of variation were assessed by performing a PERMANOVA (Anderson, 2001) using the 'adonis' function (on Euclidean distances with 999 permutations) from the R-package vegan v. 2.5–6, (Oksanen et al., 2019).

2.3.2.5. Contamination. Protein extraction blanks contained only four proteins in total: trypsin (TRYP_PIG), serum albumin (ALBU_BOVIN), collagen alpha-1 (I) chain (CO1A1), and collagen alpha-2 (I) chain (CO1A2). Porcine trypsin is a laboratory reagent used during protein digestion, but was not identified in any of the calculus samples. Bovine serum albumin is a common laboratory contaminant (www.thegpm.org/crap/), and therefore serum albumin was classified as a contaminant regardless of assigned species, although some of it is likely endogenous. While some collagen recovered from dental calculus is also likely endogenous (released from the gingiva and periodontium bone during inflammation), its frequent recovery from extraction blanks led us to classifying it as a contaminant for the purposes of this study. Keratins, although not identified in our blanks, are common laboratory contaminants (www.thegpm.org/crap/) and were classified as contaminants. The proportion of spectra in the calculus samples belonging to these proteins was compared across extraction protocols.

3. Results

3.1. Genetic analysis

3.1.1. DNA recovery

To investigate how the DO and UP protocols differ in performance for DNA extraction, we compared normalized DNA yield for both protocols (Data S1). Only choice of extraction method, not starting material mass, was found to be a significant predictor of DNA recovery, with UP having lower DNA recovery ($p < 0.001$). On average, DO10 yielded 1.8 ± 0.2 (mean ± standard deviation) fold more DNA per mg calculus than UP10, and DO2 yielded 1.7 ± 0.6 fold more than UP2 (Fig. 2). The largest decrease in yield was seen in WIG001, the sample with best estimated preservation. The poorly preserved individual RUV001 showed the opposite trend, with UP10 yielding 1.2 fold more DNA than DO10, and UP2 yielding 1.4 fold more DNA than DO2. However, RUV001 had very low DNA recovery overall, and the absolute difference in DNA recovery between the protocols was negligible (only 0.7 ng/mg on average).

3.1.2. DNA fragment characteristics

Given that there are differences in DNA recovery based on protocol, we next tested whether there are differences in the characteristics of the DNA fragments recovered by each protocol. Previous studies have shown that DNA extracted from ancient dental calculus may yield biases in microbial taxonomic profiles due to selective loss of short, AT-rich sequences (Mann et al., 2018). We calculated the mean fragment length and GC-content per sequence library from alignments to *Actinomyces oris* and *Leptotrichia buccalis* (Fig. 3). The only significant shifts observed for GC-content and fragment length were found in *A. oris*, where GC-content is significantly different between DO2 and DO10, as well as between UP2 and DO10 (pW-BH, $p < 0.05$ in both cases). In addition, a considerable shift in median fragment length can be seen among reads from our selected bacterial species, where *L. buccalis* shows median fragment lengths of 43–51 bp, whereas *A. oris* has median fragment lengths of 46–75 bp (with RUV001 excluded). The average GC-content of *L. buccalis* reads, 31.5%–34.4%, is also higher than the genome average of 29.6% (dashed grey line in Fig. 3A), which all agrees with the previously-reported loss of short, AT-rich sequences (Mann et al., 2018).

3.1.3. Microbiome reconstruction

Ancient dental calculus has been found to be dominated by oral

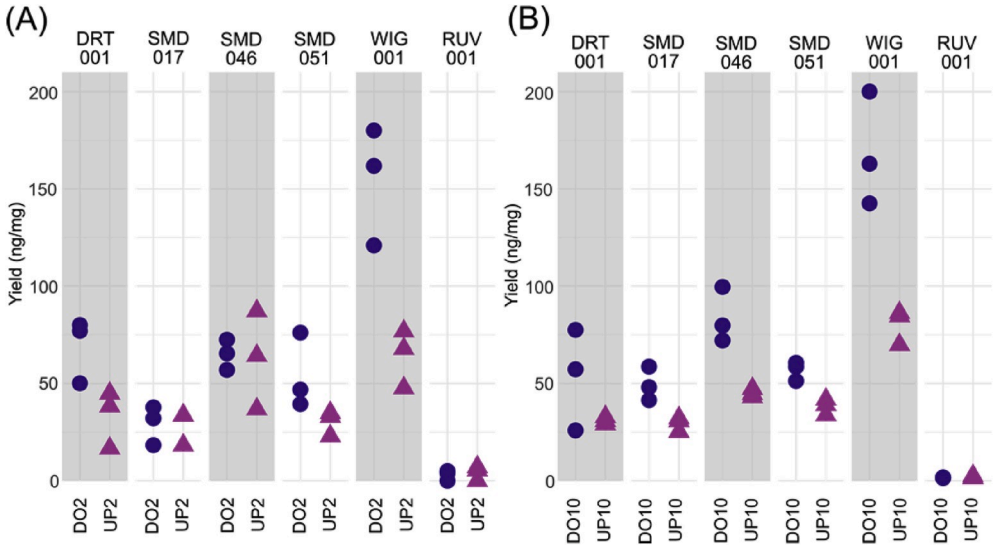

Fig. 2. DNA yield differs significantly by extraction protocol but not starting mass of dental calculus. Normalized DNA yield for triplicate extracts of (A) DO2 and UP2, and (B) DO10 and UP10, ordered by individual from oldest to most recent.

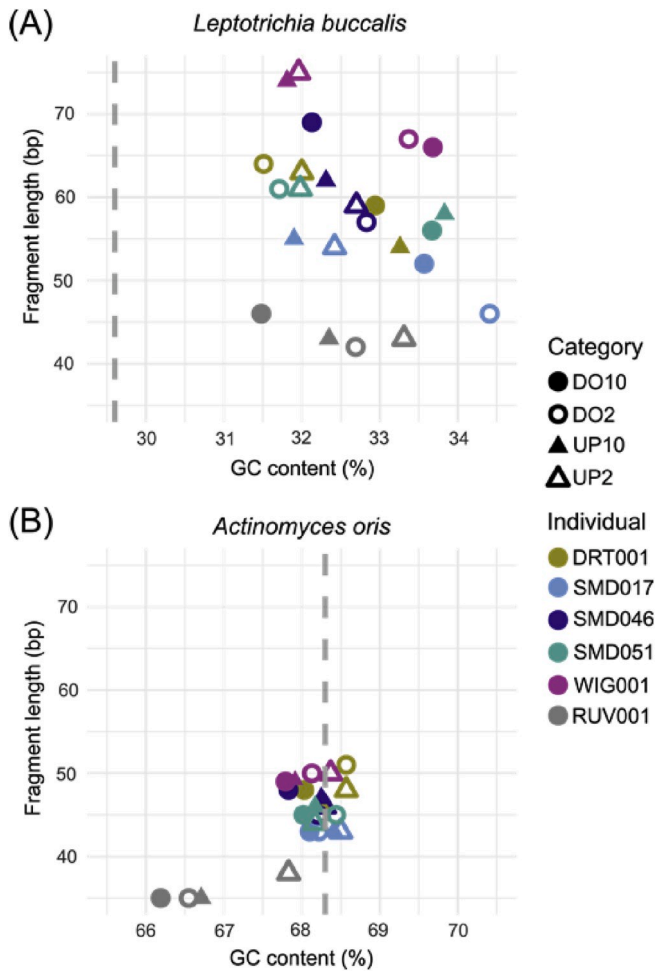

Fig. 3. Median fragment length by GC-content for (A) *L. buccalis* and (B) *A. oris* show no consistent changes by choice of extraction protocol. Dashed grey line shows expected median GC-content of genome.

bacteria from the phyla Firmicutes, Actinobacteria, Proteobacteria, and Bacteroidetes (Warinner et al., 2014b), which accords with the known composition of dental plaque biofilms today (Dewhirst et al., 2010). The DNA sequences obtained from dental calculus in this study are overwhelmingly bacterial in origin (Data S2), and these four phyla account for 83.5% of the identified bacterial species (excluding RUV001). Dental calculus from the poorly preserved individual RUV001 contains considerably more identified species (641 ± 19 species) than the other individuals (181 ± 25 species), which is consistent with RUV001 being a highly degraded sample infiltrated by diverse environmental taxa (Fig. 4A). There are no significant differences in the number of species identified between the different extraction protocols or starting weights, nor in the proportions of the four most abundant phyla (pW-BH, $p > 0.05$ in all cases). For the 20 most abundant species, the majority of which were oral species, no significant taxonomic differences were identified between the extraction protocols (pW-BH, $p > 0.05$ in all cases); rather taxonomic differences are primarily driven by individual (Fig. 4B).

A principal component analysis on genus level read counts shows no systematic shifts by extraction protocol or starting weight (Fig. 4C). The samples cluster by individual (PERMANOVA, $p < 0.001$), and the genera separating the samples are mostly environmental. This indicates that the main drivers of separation are bacteria from the burial environment. When the poorly preserved individual (RUV001) is added to the PCA (Fig. S1), it is separated from the other individuals along PC1, which also separates oral from environmental genera as the major loadings, indicating that this individual has a distinct microbial composition compared to the well-preserved samples.

3.1.4. Contamination

Contamination is a major issue for studies of ancient biomolecules, and laboratory procedures can influence contamination levels (Key et al., 2017; Salter et al., 2014; Warinner et al., 2017). We therefore assessed whether the choice of extraction protocol affects the level of estimated contamination observed for the samples. Using the R-package decontam (Davis et al., 2018), a total of 154 species were identified as putative contaminants (Data S3). Of these, the majority belong to Bacteria (n = 95) and Animalia (n = 33). Excluding RUV001, the proportion of putative contaminants averaged 0.05 ± 0.03%, ranging from 0.01% to 0.13% of total reads per extract (Fig. S2), and did not significantly differ between extraction protocols or starting weights (pW-BH, $p > 0.05$). Contamination in the poorly preserved individual, RUV001, was >100-fold higher (9.39 ± 0.36%) than in the other samples, a finding consistent with previous analysis of calculus from this site (Ziesemer et al., 2015).

3.2. Proteomic analysis

3.2.1. Protein recovery

To evaluate UP performance, we compared total protein recovery between the PO and UP protocols (Fig. 5; Data S1). The best fitting model to predict protein recovery was found to be an interaction between starting weight and protocol ($p < 0.001$). When normalized for input weight, UP2 extractions yielded 2.0 ± 0.3 fold more protein than UP10 extractions, and PO2 extractions yielded 3.2 ± 0.4 fold more protein than PO10 extractions (although in both cases absolute recovery was higher for 10 mg extractions). This pattern suggests that the FASP protocol used in this study may be limiting protein recovery efficiency at higher amounts of starting material. For the 2 mg extractions PO2 yielded 1.3 ± 0.1 fold more proteins than UP2, whereas for the 10 mg extractions the opposite pattern was observed, where UP10 yielded 1.3 ± 0.1 fold more proteins than PO10. The increase in normalized protein recovery through UP10 over PO10 may also be caused by the limitation of the amount of input material in FASP, as UP10 has a lower amount of input material (90% of the supernatant is excluded from the protein extraction). However, FASP is known to have relatively low consistency between technical replicates (Sielaff et al., 2017), and this variation may have influenced our results. In addition, protein concentration measurement may be less accurate at lower protein inputs. Further work is needed to determine whether FASP is indeed more efficient with lower input amounts of dental calculus, and to what degree other factors may be contributing to our observed pattern.

3.2.2. Protein characteristics

In the UP, only 10% of the supernatant is reserved for protein extraction. Hydrophilic proteins, which we expect to be mainly present in the supernatant, could thereby be lost to the DNA extraction fraction. Ideally, a unified protocol should not have a skewed representation of hydrophobic and/or hydrophilic proteins compared to a protein-only extraction method. To test for this potential bias, we compared the hydropathy values of proteins and physicochemical properties of each amino acid of peptides recovered using the UP and PO protocols (Data S4). The mean protein hydropathy values did not significantly differ between the two extraction protocols (pW-BH, $p > 0.05$; Fig. 6A). However, significant differences in amino acid properties were found with respect to basic amino acids (Fig. 6B), which are hydrophilic. The proportion of basic amino acids was significantly different between UP10 and PO10, UP10 and PO2, UP2 and PO10, and UP2 and PO2 (pW-BH, $p < 0.05$ in all cases), with the PO protocol consistently recovering a higher proportion of basic amino acids. Thus, the UP may result in an underrepresentation of hydrophilic proteins, particularly those containing basic residues. Further, the proportion of acidic amino acids (Fig. S3) was significantly higher in UP2 than PO10 (pW-BH, $p < 0.05$).

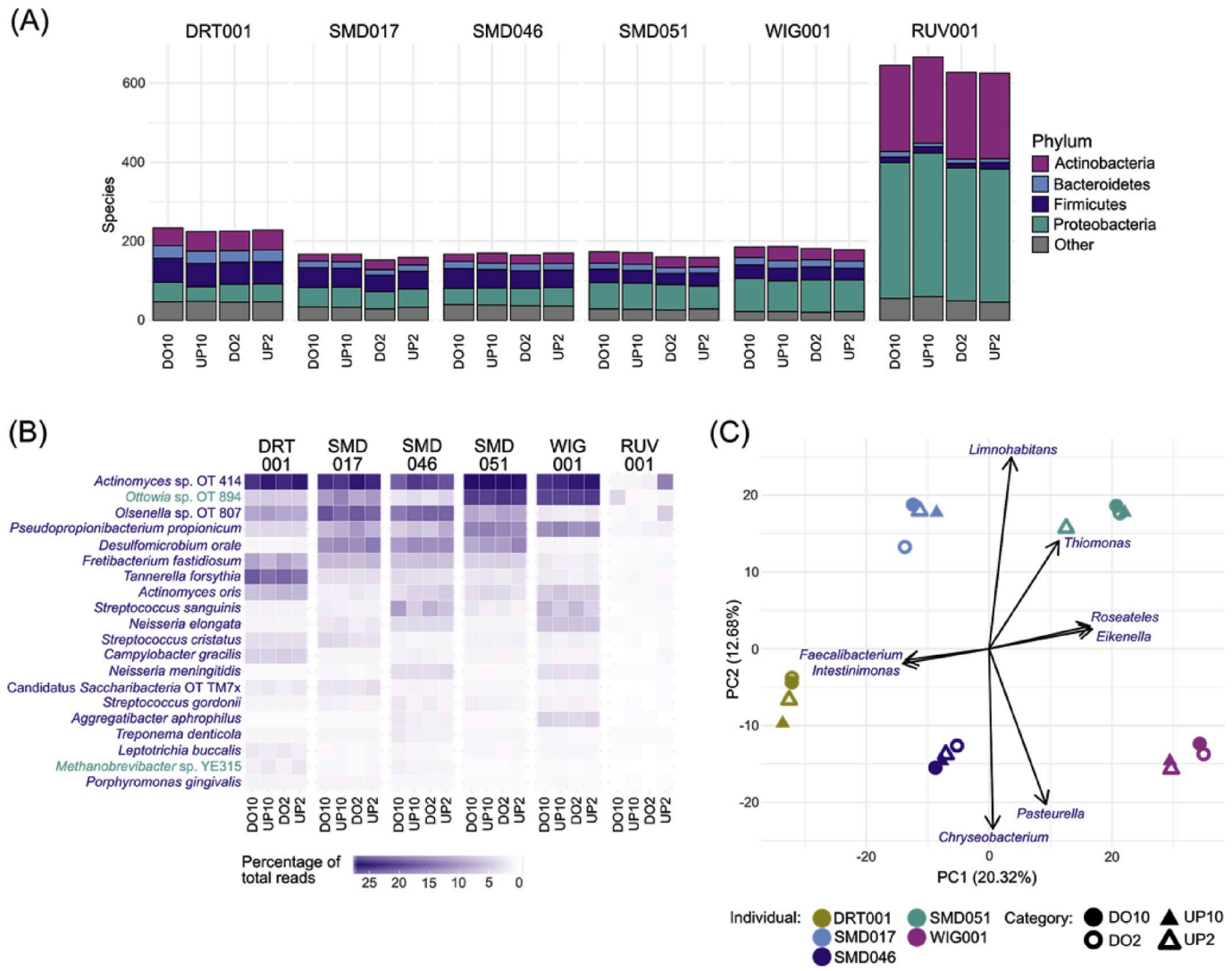

Fig. 4. Microbiome profiles are consistent between extraction protocols. (A) Number of species identified in each sample, grouped by phylum. Phyla containing <5% of total species are grouped under "Other". (B) Heatmap of percentage of total assigned reads for the 20 most abundant species, with species names colored according to if they are oral (blue) or unassigned (green) in eHOMD. OT = oral taxon. (C) PCA on genus level taxa, without individual RUV001. The top genera contributing to separation for each principal component as major loadings are indicated by arrows. (For interpretation of the references to color in this figure legend, the reader is referred to the Web version of this article.)

Finally, we tested whether the UP exhibited biases based on protein size. We found that the mean molecular weight of recovered proteins was not significantly affected by choice of extraction protocol or starting weight (pW-BH, $p > 0.05$; Fig. S4).

3.2.3. *Proteome reconstruction*

The number of identified protein clusters (Data S5) did not significantly differ by extraction protocol or starting weight (pW-BH, $p > 0.05$; Fig. 7A). The highest number of identified protein clusters (67.5 ± 9.3) was observed for WIG001, while the lowest (17.8 ± 4.3) was observed for RUV001, which is consistent with the differing preservation of these two samples. Among the identified protein clusters, most are found in various cellular locations, followed by intracellular/organelle and extracellular proteins clusters; only a small number of membrane protein clusters were identified. The choice of extraction protocol did not significantly affect the proportions of these groups (pW-BH, $p > 0.05$ in all cases). Of the 20 most abundant protein clusters, most are associated with host defenses against microbes or bacterial cellular processes (Fig. 7B). This is consistent with previous findings for modern and well-preserved ancient dental calculus (Jersie-Christensen et al., 2018; Velsko et al., 2019; Warinner et al., 2014b). Although some protein clusters seem to differ in abundance by extraction method by visual inspection, statistical significance is not reached with this design, due to the need to correct p-values for multiple testing and for the abundances being dependent.

In a principal component analysis of identified protein clusters, the samples were found to cluster by individual and extraction method (PERMANOVA, $p < 0.001$ for both), but not starting weight (Fig. 7C). The major protein cluster separating extraction protocols along PC1 is Elongation factor Tu (EFTU_NEIMA), which is involved in protein biosynthesis. It is a hydrophobic protein (hydropathy index −0.136) and would thereby be found at a higher proportion in the UP, where hydrophilic proteins are lost to the aqueous fraction. This pattern is also present in the abundance of this protein cluster (Fig. 7B). Adding RUV001 to the PCA did not considerably alter the relationships between the samples (Fig. S5).

3.2.4. *Contamination*

Of the total identified spectra per sample, 0.39–6.11% were assigned to collagen, keratin and serum albumin proteins, which were classified

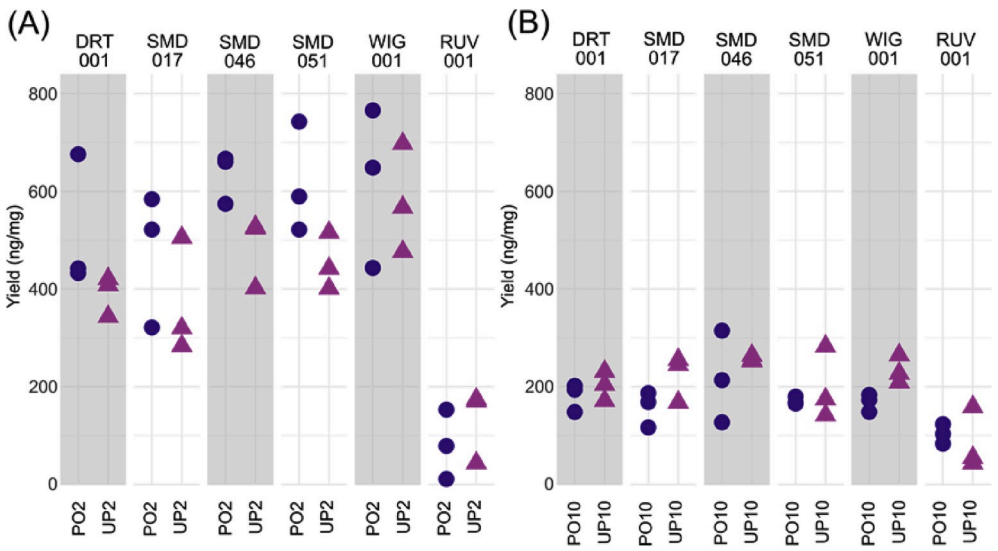

Fig. 5. Protein yield differs by starting material mass and extraction method. Protein yield normalized by sample mass for triplicate extracts of (A) PO2 and UP2, and (B) PO10 and UP10, ordered by individual from oldest to most recent.

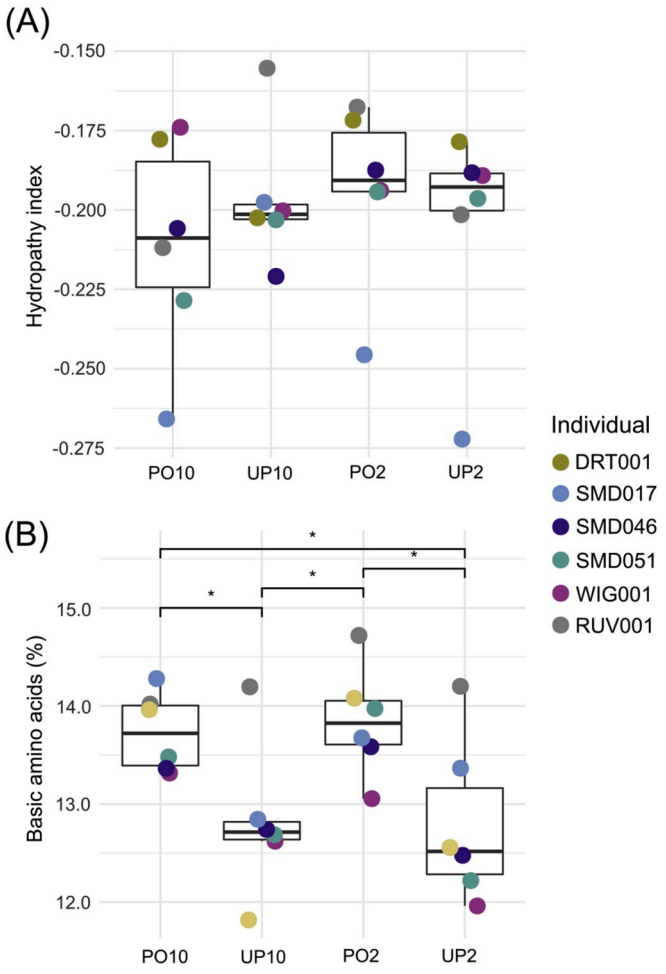

Fig. 6. Protein hydropathy is unaffected by extraction protocol, but basic amino acids may be lost in UP. (A) Hydropathy index of identified proteins. (B) Proportion of basic amino acids among recovered peptides, with significant pairwise tests indicated by brackets (*$p < 0.05$; **$p < 0.01$; ***$p < 0.001$).

as probable contaminants (Fig. S6). There was no correlation between contaminant spectra and extraction protocol or starting weight, neither overall nor in the proportions of the different contaminants (pW-BH, $p > 0.05$ in all cases).

4. Discussion and conclusions

Protocols that allow for the simultaneous extraction of different biomolecules, such as DNA and proteins, can reduce sampling demands for archaeological remains, thus supporting their long-term curation and preservation. For a unified protocol to be an acceptable alternative to simply performing two separate extractions, the unified protocol should recover at least 50% of the biomolecules that each individual protocol recovers separately. Otherwise, splitting the sample in half and performing two separate extractions will have a higher overall yield. Further, the protocol should introduce no major biases, and contamination levels should not be altered. Careful testing of protocols is therefore necessary to evaluate if all the above criteria are met.

In this study, we developed a unified protocol for the simultaneous extraction of DNA and proteins, and compared its performance to separate DNA and protein extraction protocols. During the unified protocol, archaeological dental calculus is decalcified in EDTA, and different fractions of this solution are used to recover DNA and proteins, based on the expected solubility of these biomolecules. Because ancient DNA is highly fragmented, and the sugar-phosphate backbone of DNA is negatively charged and hydrophilic, we expect the majority of DNA molecules to be present in the aqueous fraction. Proteins, on the other hand, are biochemically complex and may be very large (e.g. collagen), membrane-bound, or otherwise have reduced solubility in their native (non-denatured) state. Consequently, we expect them to mostly pellet out of solution during centrifugation of the decalcified sample. Some proteins are, however, highly hydrophilic, and therefore we included a portion (10%) of the aqueous fraction in our protein extraction. Following this initial partitioning of DNA into the aqueous supernatant and proteins into the pellet (plus a small portion of the supernatant), we proceeded to isolate each biomolecule using optimized methods.

Overall, we found that a significant amount of DNA (mean 43%) is lost in the unified protocol, presumably to the pellet, and the effect is greatest for well-preserved samples. One possible explanation for this pattern is that proteinase K is not added to the sample until after the fractions have been separated in the unified protocol, and a substantial portion of DNA may be bound to insoluble proteins or trapped within

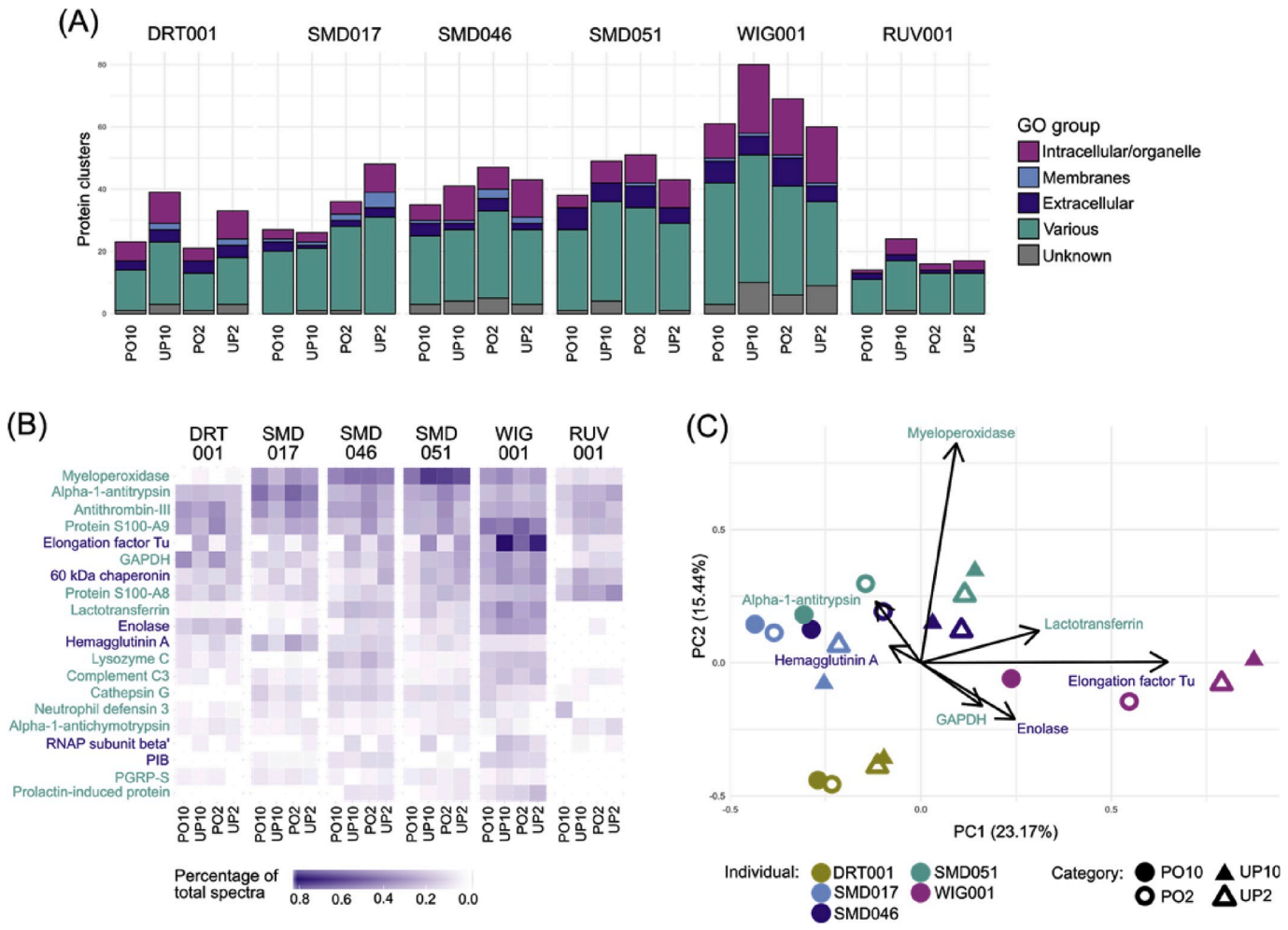

Fig. 7. Choice of extraction protocol does not induce major biases in proteome reconstruction. (A) Number of identified protein clusters per extraction protocol, colored by GO cellular location. (B) Percentage of spectra assigned to the top 20 most abundant protein clusters per sample. (C) PCA of protein clusters without RUV001, where the top protein clusters contributing to separation along each principal component as major loadings are indicated by arrows. Protein cluster names in (B) and (C) are colored according to: Blue = prokaryotes, green = eukaryotes. (For interpretation of the references to color in this figure legend, the reader is referred to the Web version of this article.)

cellular structures that are pelleted during centrifugation. In the DNA-only protocol, the entire sample is exposed to proteinase K, which breaks up proteins and cellular membranes, thereby facilitating greater DNA release. Unfortunately, this is not a problem that is easily overcome. Proteinase K cannot be added to the entire sample in the unified protocol, as this enzyme produces peptides too small for successful analysis using LC-MS/MS. On the other hand, using an alternative enzyme compatible with LC-MS/MS, such as trypsin, is not feasible due to the risk of its autodigestion when left active for an extended period of time, such as during calculus decalcification; such autodigestion can result in off-target cleavages performed by the enzyme, which reduces downstream protein identifications. Trypsin digestion during decalcification would also preclude the use of FASP for protein extraction, as this protocol relies on size exclusion to remove EDTA and other lysis components that would interfere with downstream analysis. For protein extractions, acids can be used in place of EDTA for decalcification, which may assist with pellet digestion, but even weak acids can cause DNA to undergo hydrolysis and depurination, thus making acids unsuitable for genetic analysis.

Although the unified protocol does lead to reduced DNA recovery, it is still more efficient than performing two separate biomolecular extractions. In addition, the DNA losses are mitigated by the fact that the starting amount of DNA within archaeological dental calculus is typically very high (however see Austin et al. (2019) for exceptions). For example, in a study of paired dental calculus and dentine samples, Mann et al. (2018) reported a median DNA recovery from calculus of 72.1 ng/mg compared to 4.8 ng/mg for dentin. However, given the significantly reduced DNA recovery through the unified protocol, it is advisable to keep some material aside for a potential future DNA-only extraction, especially in cases where preservation status is unknown. Beyond reducing DNA recovery, we found that the unified protocol does not affect downstream genetic analyses or change the amount of identified contaminants. Although we sequenced only one of the three extraction replicates, thereby reducing our statistical power, the results are consistent over multiple individuals, and thus appear generalizable.

Protein recovery using the unified protocol was significantly different from the protein-only protocol, but recovery was only decreased by 20.6% on average for the 2 mg extractions, confirming that the majority of proteins are present in the initial cell debris pellet. For the 10 mg extractions, on the other hand, protein recovery was surprisingly increased (mean 25.3%) through the unified protocol. Equally unexpectedly, protein recovery (normalized by weight of input material) was found to be higher when using 2 mg of starting material than when using 10 mg, a trend that was not reflected in DNA extractions. This suggests that the version of the FASP protocol used for protein purification may be limiting protein yield at higher amounts of input material. This also explains the increase in recovery through the unified protocol when using 10 mg starting material, as the amount of input

material is lower in the unified protocol (where only 10% of the supernatant is used for protein extraction) than in the protein-only protocol. However, it is not clear from our results what the limiting factor in the FASP protocol could be, and overall, we observed a high variance in protein recovery. FASP has a relatively high variability between technical replicates (Sielaff et al., 2017), which may cause the variance in our results. Further, spectrophotometric measurements of peptide bonds at 215 nm absorbance can have a high error rate if other organic compounds have not been sufficiently removed, which is possible here given the complex nature of dental calculus and the variety of chemicals used in FASP. Aside from protein recovery, there were no observable differences in downstream analyses between the two starting material weights.

In addition to the difference in protein recovery between the protocols, a significantly lower proportion of basic amino acids among downstream identified peptides was observed through the unified protocol, suggesting that the unified protocol may have a slight bias against hydrophilic proteins. The bias is likely minor, as no difference in overall hydropathy of proteins was observed. However, if a specific, hydrophilic protein is the target of a research study, further testing is recommended before implementing the unified protocol.

Although most dental calculus samples in this study exhibited good biomolecular preservation, the 19th century Rupert's Valley dental calculus was known to be poorly preserved, and it performed differently than the other samples in most analyses. It was previously reported to have poor DNA preservation and high contamination by environmental bacteria (Ziesemer et al., 2015), which we likewise observed in our genetic analyses. However, our protein analyses did not show high levels of environmental bacteria. Instead, fewer protein clusters were identified than in other samples, likely due to a lack of sufficient representation of environmental bacteria in the protein database. It is therefore important to note that choice of database may affect assessment of sample preservation.

Moving forward, it may be possible to combine the unified protocol with palaeoethnobotanical and other microparticle analyses. Recently, it was shown that microparticle recovery from dental calculus following EDTA decalcification is both possible and more successful compared to conventional decalcification using HCl (Tromp et al., 2017). During the unified protocol, a visible pellet of insoluble cell debris often remains after DNA and protein extraction, and recovery of microparticles may be possible, especially for phytoliths, which are not damaged by the heating step during protein extraction. Extending the unified protocol to also incorporate microremains will further broaden the range of information that can be obtained from a single sample of dental calculus, while further decreasing destructive demands on this valuable archaeological resource.

Accession numbers

Genetic data have been deposited in the ENA under the accession PRJEB35483. Raw and processed LC-MS/MS data files have been deposited in the ProteomeXchange Consortium via the PRIDE partner repository under the identifier PXD015817.

Author contributions

Z.F., C.S., J.H., and C.W. designed the study. C.S. and J.H. conceived of the unified protocol. Z.F. performed the experiments. Z.F. analyzed the data. M.I.G.C., C.S., J.H., and C.A.H. provided materials and resources. Z.F. wrote the manuscript with input from C.W., I.V. and the other authors.

Declaration of competing interest

The authors declare that they have no known competing financial interests or personal relationships that could have appeared to influence the work reported in this paper.

Acknowledgements

This work was supported by the US National Science Foundation (BCS-1516633, BCS-1528698 to C.W., and BCS-1643318 to C.W. and C. H.), the Max Planck Society, and the Government of the Basque Country (IT1193-19). The authors thank Franziska Aron, Raphaela Stahl, and Richard Hagan for laboratory assistance, and James Fellows Yates, A. Ben Rohrlach, Alexander Hübner, and Ashley Scott for assistance with data analysis. The authors also thank the personnel at the Functional Genomics Centre Zürich for their assistance with data generation. We thank York Archaeological Trust for Excavation and Research Ltd (Christine McDonnell), York Osteoarchaeology Ltd (Malin Holst, Katie Keefe), Andrew Pearson, and Iterbide S.C. (Javier Niso, Miguel Loza) for providing access to skeletal collections.

Appendix A. Supplementary data

Supplementary data to this article can be found online at https://doi.org/10.1016/j.jas.2020.105135.

References

Ahlmann-Eltze, C., 2019. ggsignif: significance Brackets for "ggplot2.". https://CRAN.R-project.org/package=ggsignif.
Anderson, M.J., 2001. A new method for non-parametric multivariate analysis of variance: non-parametric manova for ecology. Austral Ecol. 26, 32–46.
Austin, R.M., Sholts, S.B., Williams, L., Kistler, L., Hofman, C.A., 2019. Opinion: to curate the molecular past, museums need a carefully considered set of best practices. Proc. Natl. Acad. Sci. U. S. A 116, 1471–1474.
Bates, D., Mächler, M., Bolker, B., Walker, S., 2015. Fitting linear mixed-effects models using lme4. J. Stat. Software 67.
Berstan, R., Stott, A.W., Minnitt, S., Bronk Ramsey, C., Hedges, R.E.M., Evershed, R.P., 2008. Direct dating of pottery from its organic residues: new precision using compound-specific carbon isotopes. Antiquity 82, 702–713.
Bolnick, D.A., Bonine, H.M., Mata-Míguez, J., Kemp, B.M., Snow, M.H., LeBlanc, S.A., 2012. Nondestructive sampling of human skeletal remains yields ancient nuclear and mitochondrial DNA. Am. J. Phys. Anthropol. 147, 293–300.
Casanova, E., Knowles, T.D.J., Williams, C., Crump, M.P., Evershed, R.P., 2018. Practical considerations in high-precision compound-specific radiocarbon analyses: eliminating the effects of solvent and sample cross-contamination on accuracy and precision. Anal. Chem. 90, 11025–11032.
Chen, F., Welker, F., Shen, C.-C., Bailey, S.E., Bergmann, I., Davis, S., Xia, H., Wang, H., Fischer, R., Freidline, S.E., Yu, T.-L., Skinner, M.M., Stelzer, S., Dong, G., Fu, Q., Dong, G., Wang, J., Zhang, D., Hublin, J.-J., 2019. A late middle pleistocene denisovan mandible from the Tibetan plateau. Nature 569, 409–412.
Dabney, J., Knapp, M., Glocke, I., Gansauge, M.-T., Weihmann, A., Nickel, B., Valdiosera, C., García, N., Pääbo, S., Arsuaga, J.-L., Meyer, M., 2013. Complete mitochondrial genome sequence of a Middle Pleistocene cave bear reconstructed from ultrashort DNA fragments. Proc. Natl. Acad. Sci. U. S. A 110, 15758–15763.
Davis, N.M., Proctor, D.M., Holmes, S.P., Relman, D.A., Callahan, B.J., 2018. Simple statistical identification and removal of contaminant sequences in marker-gene and metagenomics data. Microbiome 6, 226.
Demarchi, B., Hall, S., Roncal-Herrero, T., Freeman, C.L., Woolley, J., Crisp, M.K., Wilson, J., Fotakis, A., Fischer, R., Kessler, B.M., Rakownikow Jersie-Christensen, R., Olsen, J.V., Haile, J., Thomas, J., Marean, C.W., Parkington, J., Presslee, S., Lee-Thorp, J., Ditchfield, P., Hamilton, J.F., Ward, M.W., Wang, C.M., Shaw, M.D., Harrison, T., Domínguez-Rodrigo, M., MacPhee, R.D.E., Kwekason, A., Ecker, M., Kolska Horwitz, L., Chazan, M., Kröger, R., Thomas-Oates, J., Harding, J.H., Cappellini, E., Penkman, K., Collins, M.J., 2016. Protein sequences bound to mineral surfaces persist into deep time. Elife 5.
Dewhirst, F.E., Chen, T., Izard, J., Paster, B.J., Tanner, A.C.R., Yu, W.-H., Lakshmanan, A., Wade, W.G., 2010. The human oral microbiome. J. Bacteriol. 192, 5002–5017.
Escapa, I.F., Chen, T., Huang, Y., Gajare, P., Dewhirst, F.E., Lemon, K.P., 2018. New insights into human nostril microbiome from the expanded human oral microbiome database (eHOMD): a resource for the microbiome of the human aerodigestive tract. mSystems 3.
Fiddyment, S., Holsinger, B., Ruzzier, C., Devine, A., Binois, A., Albarella, U., Fischer, R., Nichols, E., Curtis, A., Cheese, E., Teasdale, M.D., Checkley-Scott, C., Milner, S.J., Rudy, K.M., Johnson, E.J., Vnouček, J., Garrison, M., McGrory, S., Bradley, D.G., Collins, M.J., 2015. Animal origin of 13th-century uterine vellum revealed using noninvasive peptide fingerprinting. Proc. Natl. Acad. Sci. U. S. A 112, 15066–15071.
Firke, S., 2018. Janitor: simple tools for examining and cleaning dirty data. https://CRAN.R-project.org/package=janitor.
Gloor, G.B., Macklaim, J.M., Pawlowsky-Glahn, V., Egozcue, J.J., 2017. Microbiome datasets are compositional: and this is not optional. Front. Microbiol. 8, 2224.

Green, E.J., Speller, C.F., 2017. Novel substrates as sources of ancient DNA: prospects and hurdles. Genes 8.
Hendy, J., Warinner, C., Bouwman, A., Collins, M.J., Fiddyment, S., Fischer, R., Hagan, R., Hofman, C.A., Holst, M., Chaves, E., Klaus, L., Larson, G., Mackie, M., McGrath, K., Mundorff, A.Z., Radini, A., Rao, H., Trachsel, C., Velsko, I.M., Speller, C.F., 2018. Proteomic evidence of dietary sources in ancient dental calculus. Proc. Biol. Sci. 285.
Henry, A.G., Piperno, D.R., 2008. Using plant microfossils from dental calculus to recover human diet: a case study from Tell al-Raqā'i, Syria. J. Archaeol. Sci. 35, 1943–1950.
Herbig, A., Maixner, F., Bos, K.I., Zink, A., Krause, J., Huson, D.H., 2016. MALT: Fast Alignment and Analysis of Metagenomic DNA Sequence Data Applied to the Tyrolean Iceman (bioRxiv).
Huson, D.H., Beier, S., Flade, I., Górska, A., El-Hadidi, M., Mitra, S., Ruscheweyh, H.-J., Tappu, R., 2016. MEGAN community edition - interactive exploration and analysis of large-scale microbiome sequencing data. PLoS Comput. Biol. 12, e1004957.
Jeong, C., Wilkin, S., Amgalantugs, T., Bouwman, A.S., Taylor, W.T.T., Hagan, R.W., Bromage, S., Tsolmon, S., Trachsel, C., Grossmann, J., Littleton, J., Makarewicz, C. A., Krigbaum, J., Burri, M., Scott, A., Davaasambuu, G., Wright, J., Irmer, F., Myagmar, E., Boivin, N., Robbeets, M., Rühli, F.J., Krause, J., Frohlich, B., Hendy, J., Warinner, C., 2018. Bronze Age population dynamics and the rise of dairy pastoralism on the eastern Eurasian steppe. Proc. Natl. Acad. Sci. U. S. A 115, E11248–E11255.
Jersie-Christensen, R.R., Lanigan, L.T., Lyon, D., Mackie, M., Belstrøm, D., Kelstrup, C.D., Fotakis, A.K., Willerslev, E., Lynnerup, N., Jensen, L.J., Cappellini, E., Olsen, J.V., 2018. Quantitative metaproteomics of medieval dental calculus reveals individual oral health status. Nat. Commun. 9, 4744.
Kassambara, A., 2018. Ggpubr: "ggplot2" based publication ready plots. https://CRAN.R-project.org/package=ggpubr.
Key, F.M., Posth, C., Krause, J., Herbig, A., Bos, K.I., 2017. Mining metagenomic data sets for ancient DNA: recommended protocols for authentication. Trends Genet. 33, 508–520.
Kircher, M., Sawyer, S., Meyer, M., 2012. Double indexing overcomes inaccuracies in multiplex sequencing on the Illumina platform. Nucleic Acids Res. 40, e3.
Korlević, P., Talamo, S., Meyer, M., 2018. A combined method for DNA analysis and radiocarbon dating from a single sample. Sci. Rep. 8, 4127.
Kuznetsova, A., Brockhoff, P.B., Christensen, R.H.B., 2017. lmerTest package: tests in linear mixed effects models. J. Stat. Software 82.
Li, H., Durbin, R., 2009. Fast and accurate short read alignment with Burrows-Wheeler transform. Bioinformatics 25, 1754–1760.
Li, H., Handsaker, B., Wysoker, A., Fennell, T., Ruan, J., Homer, N., Marth, G., Abecasis, G., Durbin, R., 1000 Genome Project Data Processing Subgroup, 2009. The sequence alignment/map format and SAMtools. Bioinformatics 25, 2078–2079.
Mackie, M., Radini, A., Speller, C.F., 2017. The sustainability of dental calculus for archaeological research. In: Favreau, J., Patalano, R. (Eds.), Shallow Pasts, Endless Horiozons: Sustainability & Archaeology:Proceedings of the 48th Annual Chacmool Archaeology Conference, p. 8.
Manfredi, M., Barberis, E., Gosetti, F., Conte, E., Gatti, G., Mattu, C., Robotti, E., Zilberstein, G., Koman, I., Zilberstein, S., Marengo, E., Righetti, P.G., 2017. Method for noninvasive analysis of proteins and small molecules from ancient objects. Anal. Chem. 89, 3310–3317.
Mann, A.E., Sabin, S., Ziesemer, K., Vågene, Å.J., Schroeder, H., Ozga, A.T., Sankaranarayanan, K., Hofman, C.A., Fellows Yates, J.A., Salazar-García, D.C., Frohlich, B., Aldenderfer, M., Hoogland, M., Read, C., Milner, G.R., Stone, A.C., Lewis Jr., C.M., Krause, J., Hofman, C., Bos, K.I., Warinner, C., 2018. Differential preservation of endogenous human and microbial DNA in dental calculus and dentin. Sci. Rep. 8, 9822.
Meyer, M., Kircher, M., 2010. Illumina sequencing library preparation for highly multiplexed target capture and sequencing. Cold Spring Harb. Protoc. 2010 db.prot5448.
Nowosad, J., 2018. CARTOColors' palettes. https://nowosad.github.io/rcartocolor.
Oksanen, J., Blanchet, F.G., Friendly, M., Kindt, R., Legendre, P., McGlinn, D., Minchin, P.R., O'Hara, R.B., Simpson, G.L., Solymos, P., Stevens, M.H.H., Szoecs, E., Wagner, H., 2019. Vegan: community ecology package. https://CRAN.R-project.org/package=vegan.
Orlando, L., Ginolhac, A., Zhang, G., Froese, D., Albrechtsen, A., Stiller, M., Schubert, M., Cappellini, E., Petersen, B., Moltke, I., Johnson, P.L.F., Fumagalli, M., Vilstrup, J.T., Raghavan, M., Korneliussen, T., Malaspinas, A.-S., Vogt, J., Szklarczyk, D., Kelstrup, C.D., Vinther, J., Dolocan, A., Stenderup, J., Velazquez, A.M.V., Cahill, J., Rasmussen, M., Wang, X., Min, J., Zazula, G.D., Seguin-Orlando, A., Mortensen, C., Magnussen, K., Thompson, J.F., Weinstock, J., Gregersen, K., Røed, K.H., Eisenmann, V., Rubin, C.J., Miller, D.C., Antczak, D.F., Bertelsen, M.F., Brunak, S., Al-Rasheid, K.A.S., Ryder, O., Andersson, L., Mundy, J., Krogh, A., Gilbert, M.T.P., Kjær, K., Sicheritz-Ponten, T., Jensen, L.J., Olsen, J.V., Hofreiter, M., Nielsen, R., Shapiro, B., Wang, J., Willerslev, E., 2013. Recalibrating Equus evolution using the genome sequence of an early Middle Pleistocene horse. Nature 499, 74–78.
Osorio, D., 2015. Peptides: a package for data mining of antimicrobial peptides. R J 7, 4–14.
Ozga, A.T., Nieves-Colón, M.A., Honap, T.P., Sankaranarayanan, K., Hofman, C.A., Milner, G.R., Lewis Jr., C.M., Stone, A.C., Warinner, C., 2016. Successful enrichment and recovery of whole mitochondrial genomes from ancient human dental calculus. Am. J. Phys. Anthropol. 160, 220–228.
Palarea-Albaladejo, J., Martín-Fernández, J.A., 2015. zCompositions — R package for multivariate imputation of left-censored data under a compositional approach. Chemometr. Intell. Lab. Syst. 143, 85–96.
Peltzer, A., Jäger, G., Herbig, A., Seitz, A., Kniep, C., Krause, J., Nieselt, K., 2016. EAGER: efficient ancient genome reconstruction. Genome Biol. 17, 60.
Radini, A., Nikita, E., Buckley, S., Copeland, L., Hardy, K., 2017. Beyond food: the multiple pathways for inclusion of materials into ancient dental calculus. Am. J. Phys. Anthropol. 162 (Suppl. 63), 71–83.
Radini, A., Tromp, M., Beach, A., Tong, E., Speller, C., McCormick, M., Dudgeon, J.V., Collins, M.J., Rühli, F., Kröger, R., Warinner, C., 2019. Medieval women's early involvement in manuscript production suggested by lapis lazuli identification in dental calculus. Sci. Adv. 5 eaau7126.
R Core Team, 2018. R: A Language and Environment for Statistical Computing. R Foundation for Statistical Computing, Vienna, Austria. https://www.R-project.org/.
Robinson, D., 2018. Fuzzyjoin: Join Tables Together on Inexact Matching. https://CRAN.R-project.org/package=fuzzyjoin.
Rohland, N., Harney, E., Mallick, S., Nordenfelt, S., Reich, D., 2015. Partial uracil–DNA – glycosylase treatment for screening of ancient DNA. Phil. Trans. R. Soc. B 370 (20130624).
Rohland, N., Siedel, H., Hofreiter, M., 2004. Nondestructive DNA extraction method for mitochondrial DNA analyses of museum specimens. Biotechniques 36, 814–816, 818–821.
Rusu, I., Paica, I., Vulpoi, A., Radu, C., Mircea, C., Dobrinescu, C., Bodolică, V., Kelemen, B., 2019. Dual DNA-protein extraction from human archeological remains. Archaeol. Anthropol. Sci. 11, 3299–3307.
Salter, S.J., Cox, M.J., Turek, E.M., Calus, S.T., Cookson, W.O., Moffatt, M.F., Turner, P., Parkhill, J., Loman, N.J., Walker, A.W., 2014. Reagent and laboratory contamination can critically impact sequence-based microbiome analyses. BMC Biol. 12, 87.
Schubert, M., Lindgreen, S., Orlando, L., 2016. AdapterRemoval v2: rapid adapter trimming, identification, and read merging. BMC Res. Notes 9, 88.
Sielaff, M., Kuharev, J., Bohn, T., Hahlbrock, J., Bopp, T., Tenzer, S., Distler, U., 2017. Evaluation of FASP, SP3, and iST protocols for proteomic sample preparation in the low microgram range. J. Proteome Res. 16, 4060–4072.
Tromp, M., Buckley, H., Geber, J., Matisoo-Smith, E., 2017. EDTA decalcification of dental calculus as an alternate means of microparticle extraction from archaeological samples. J. Archaeol. Sci. Rep. 14, 461–466.
van Doorn, N.L., Hollund, H., Collins, M.J., 2011. A novel and non-destructive approach for ZooMS analysis: ammonium bicarbonate buffer extraction. Archaeol. Anthropol. Sci. 3, 281.
Velsko, I.M., Fellows Yates, J.A., Aron, F., Hagan, R.W., Frantz, L.A.F., Loe, L., Martinez, J.B.R., Chaves, E., Gosden, C., Larson, G., Warinner, C., 2019. Microbial differences between dental plaque and historic dental calculus are related to oral biofilm maturation stage. Microbiome 7, 102.
Velsko, I.M., Overmyer, K.A., Speller, C., Klaus, L., Collins, M.J., Loe, L., Frantz, L.A.F., Sankaranarayanan, K., Lewis Jr., C.M., Martinez, J.B.R., Chaves, E., Coon, J.J., Larson, G., Warinner, C., 2017. The dental calculus metabolome in modern and historic samples. Metabolomics 13, 134.
Velsko, I.M., Warinner, C., 2017. Bioarchaeology of the human microbiome. Bioarchaeol. Int. 1, 86–99.
Venables, W.N., Ripley, B.D., 2002. Modern Applied Statistics with S. Springer Publishing Company, Incorporated.
Warinner, C., 2016. Dental calculus and the evolution of the human oral microbiome. J. Calif. Dent. Assoc. 44, 411–420.
Warinner, C., Hendy, J., Speller, C., Cappellini, E., Fischer, R., Trachsel, C., Arneborg, J., Lynnerup, N., Craig, O.E., Swallow, D.M., Fotakis, A., Christensen, R.J., Olsen, J.V., Liebert, A., Montalva, N., Fiddyment, S., Charlton, S., Mackie, M., Canci, A., Bouwman, A., Rühli, F., Gilbert, M.T.P., Collins, M.J., 2014a. Direct evidence of milk consumption from ancient human dental calculus. Sci. Rep. 4, 7104.
Warinner, C., Herbig, A., Mann, A., Fellows Yates, J.A., Weiß, C.L., Burbano, H.A., Orlando, L., Krause, J., 2017. A robust framework for microbial archaeology. Annu. Rev. Genom. Hum. Genet. 18, 321–356.
Warinner, C., Rodrigues, J.F.M., Vyas, R., Trachsel, C., Shved, N., Grossmann, J., Radini, A., Hancock, Y., Tito, R.Y., Fiddyment, S., Speller, C., Hendy, J., Charlton, S., Luder, H.U., Salazar-García, D.C., Eppler, E., Seiler, R., Hansen, L.H., Castruita, J.A. S., Barkow-Oesterreicher, S., Teoh, K.Y., Kelstrup, C.D., Olsen, J.V., Nanni, P., Kawai, T., Willerslev, E., von Mering, C., Lewis Jr., C.M., Collins, M.J., Gilbert, M.T. P., Rühli, F., Cappellini, E., 2014b. Pathogens and host immunity in the ancient human oral cavity. Nat. Genet. 46, 336–344.
Warnes, G.R., Bolker, B., Lumley, T., 2018. Gtools: various R programming tools. https://CRAN.R-project.org/package=gtools.
Wickham, H., 2017. Tidyverse: easily install and load the "tidyverse". https://CRAN.R-project.org/package=tidyverse.
Wilke, C.O., 2017. Cowplot: streamlined plot theme and plot annotations for "ggplot2". https://CRAN.R-project.org/package=cowplot.
Wiśniewski, J.R., Zougman, A., Nagaraj, N., Mann, M., 2009. Universal sample preparation method for proteome analysis. Nat. Methods 6, 359–362.
Ziesemer, K.A., Mann, A.E., Sankaranarayanan, K., Schroeder, H., Ozga, A.T., Brandt, B. W., Zaura, E., Waters-Rist, A., Hoogland, M., Salazar-García, D.C., Aldenderfer, M., Speller, C., Hendy, J., Weston, D.A., MacDonald, S.J., Thomas, G.H., Collins, M.J., Lewis, C.M., Hofman, C., Warinner, C., 2015. Intrinsic challenges in ancient microbiome reconstruction using 16S rRNA gene amplification. Sci. Rep. 5, 16498.
Ziesemer, K.A., Ramos-Madrigal, J., Mann, A.E., Brandt, B.W., Sankaranarayanan, K., Ozga, A.T., Hoogland, M., Hofman, C.A., Salazar-García, D.C., Frohlich, B., Milner, G.R., Stone, A.C., Aldenderfer, M., Lewis Jr., C.M., Hofman, C.L., Warinner, C., Schroeder, H., 2019. The efficacy of whole human genome capture on ancient dental calculus and dentin. Am. J. Phys. Anthropol. 168, 496–509.